Self-assembled rows of Ni porphyrin dimers on the Ag(111) surface

Sergey A. Krasnikov,*[a] Natalia N. Sergeeva,[b] Yulia N. Sergeeva,[b] Mathias O. Senge[b] and Attilio A. Cafolla[a]

Received 15th October 2009, Accepted 5th March 2010
First published as an Advance Article on the web 13th April 2010
DOI: 10.1039/b921656a

The growth and ordering of 5-(10,15,20-triphenylporphyrinatonickel(II))dimer (NiTPP-dimer) molecules on the Ag(111) surface have been investigated using scanning tunnelling microscopy/spectroscopy (STM/STS) and low-energy electron diffraction (LEED). At one monolayer (ML) coverage the NiTPP-dimer forms a well-ordered close-packed molecular layer in which the porphyrin molecules have a flat orientation with the molecular plane lying parallel to the substrate. STM and LEED data obtained from one monolayer of the NiTPP-dimer on the Ag(111) surface show the formation of three domains which grow along the main crystallographic directions of the substrate. Scanning tunnelling spectroscopy data obtained from the NiTPP-dimer on the Ag(111) surface show good agreement with optical band gap measurements and density functional theory calculations.

Introduction

In the past decade there has been increasing scientific interest in the study of interface formation between organic molecules and inorganic surfaces. It is accepted that the performance of future molecular-electronic devices will depend strongly on the advances now being made in the fundamental understanding of the physical and chemical phenomena taking place at these interfaces. These include, for example, charge injection mechanisms between metal electrodes and organic layers, conducting properties, carrier recombination, molecular recognition and nonlinear optical properties.[1,2] The importance of conjugated organic molecules as new materials for molecular electronics, optoelectronics, energy conversion and gas-sensing, arises from the possibility of tuning their wide range of physical properties during chemical synthesis.[3] For example, their inherent electronic properties, such as the HOMO–LUMO gap, can be tuned by appropriate functionalisation, by doping, or by tailoring the geometric properties of molecular nanostructures.[4] More recently, the possibility of constructing novel low dimensional systems based on self-assembled functionalised organic molecules has further stimulated the surface science community to obtain a deeper understanding of intermolecular and molecule-substrate interactions.[5–7]

When molecules are deposited on a surface the interaction mechanism and the resulting physical properties of the hybrid system depend on a number of factors, such as the molecule/substrate energy level alignment, the formation of molecular resonances and their interaction with the substrate continuum, the formation of new chemical bonds which is often accompanied by charge transfer to or from the substrate, and the consequent redistribution of charge within the molecule.[8,9] Both the fundamental interest in these systems and the promise of technological applications has motivated a strong research effort in understanding and controlling these properties. It is thus imperative that the fundamental physio-chemical properties of organic molecules adsorbed on surfaces are studied in detail in order to identify new functionalities that may be exploited in nanoscale devices.[10]

Porphyrins are a ubiquitous class of naturally occurring molecules involved in a wide variety of important biological processes ranging from oxygen transport to photosynthesis and from catalysis to pigmentation changes.[3,11] Given the capability of porphyrins to bind and release gases and to act as an active center in catalytic reactions in biological systems, porphyrin-based films on surfaces are extremely appealing as chemical and gas sensors as well as nanoporous catalytic materials in novel synthetic bio-mimetic devices.[12–14] Moreover, the role of porphyrins in photosynthetic mechanisms indicates a good ability of these molecules to mediate visible photon-electron energy transfer processes.[15] For this reason metallo-porphyrins and porphyrin-substrate systems (in particular on Au, Ag, Cu, Si, Ge, TiO_2) are of major interest for applications in opto-electronics, data storage, solar cells and gas sensors[16] and an increasing number of porphyrin based assemblies have been studied for these purposes.[7,17] In turn, conjugated porphyrin oligomers such as dimers and trimers[15,16] display outstanding characteristics in many applications, including two-photon absorption,[18] reverse-saturable absorption in the near-infrared[19] and single-molecule conductivity.[20] In order to understand and exploit these properties in molecular devices the self-assembly of 3d metal porphyrin dimers recently has attracted much interest.[21]

In the present work by using STM and LEED we focus for the first time on the molecular self-assembly of the 5-(10,15,20-triphenylporphyrinatonickel(II))dimer on the Ag(111) surface in the submonolayer to one monolayer regimes in order to reveal the conformational behaviour of NiTPP-dimer

[a] *School of Physical Sciences, Dublin City University, Glasnevin, Dublin 9, Ireland. E-mail: Sergey.Krasnikov@dcu.ie; Fax: 00353 1 7005384; Tel: 00353 1 7005732*
[b] *SFI Tetrapyrrole Laboratory, School of Chemistry, Trinity College Dublin, Dublin 2, Ireland*

molecules. STS is utilised to obtain information about the local density of states. The results of this work yield important information about the electronic and structural properties of the NiTPP-dimer molecules adsorbed on the Ag(111) surface.

Experimental section

The STM/STS experiments were performed at room temperature (RT), using a commercial instrument (Omicron Nanotechnology GmbH), in an ultra-high-vacuum (UHV) system consisting of an analysis chamber (with a base pressure of 2×10^{-11} mbar) and a preparation chamber (8×10^{-11} mbar) connected to the main chamber through a gate valve. An electrochemically etched polycrystalline tungsten tip was used to record STM images in constant current mode. The voltage V_{sample} corresponds to the sample bias with respect to the tip. No drift corrections have been applied to any of the STM images presented in this paper. A single-crystal Ag(111) surface (Surface Preparation Laboratory) was used as a substrate. The Ag(111) crystal was cleaned *in situ* by repeated cycles of argon ion sputtering ($U = 1$ kV) and annealing at 820 K for 20 min until a LEED pattern with sharp diffraction spots was obtained.

The NiTPP-dimer was evaporated in a preparation chamber isolated from the STM chamber at a rate of about 0.1 ML (monolayer) per minute from a tantalum crucible in a homemade deposition cell operated at a temperature of approximately 650 K. The Ag(111) substrate was maintained at room temperature during NiTPP-dimer deposition. The total pressure during porphyrin deposition was in the 10^{-10} mbar range. Before evaporation the NiTPP-dimer powder was degassed at approximately 500 K for about 10 h to remove water vapour.

Tunnelling spectra were acquired on a grid of specified points within an image. At each grid point the scan is interrupted during imaging; the feedback loop is switched off for $I(V)$ spectroscopy and, after a short delay time to allow for stabilisation of the current preamplifier, a voltage ramp is applied. In between the grid points the feedback is on and the STM operates in constant current mode. While recording $I(V)$ spectra it was ensured that current measurements did not exceed the dynamic range of the current preamplifier. For $z(V)$ spectroscopy the feedback is on while the voltage ramp is applied. In this case the tip height is recorded as it approaches or retracts from the surface in order to maintain a constant tunnel current. Sudden changes in the $z(V)$ spectra are observed when new tunnelling channels become available, or if the tip is close enough to the surface to form chemical bonds with the molecular layer or substrate. Before and after $I(V)$ or $z(V)$ spectra acquisition the quality of the surface was verified by STM imaging to ensure that the molecular layer remained intact and no damage was done to it during the spectroscopy measurement.

5-(10,15,20-Triphenylporphyrinatonickel(II))dimer

5,15-Diphenylporphyrin (100 mg, 0.216 mmol) was dissolved in minimum amount of anhydrous THF (*ca.* 20 cm^3) and PhLi (0.72 cm^3 of 1.8 M in di-n-butyl ether) was added at RT under argon. The stirring was continued for 1 h (TLC-control) and the reaction was neutralised with ammonium chloride saturated solution (2 cm^3) followed by addition of DDQ (196 mg, 0.864 mmol). The mixture was stirred for another 30 min, then filtered *via* a silica gel plug eluted with dichloromethane (*ca.* 200 cm^3) and dried over Na_2SO_4. The solvents were removed in vacuum and a residue was recrystallised from dichloromethane–MeOH to give 5-(10,15,20-triphenylporphyrin)dimer as a brown-violet solid (93 mg, 80%). Metallation with Ni(acac)$_2$ (89 mg, 0.346 mmol) was performed in toluene (150 cm^3) at 110 °C, the progress of the reaction was monitored by TLC-control. The mixture was filtered *via* silica gel plug eluted with dichloromethane (*ca.* 200 cm^3), and concentrated in vacuum. The residue was recrystallised from dichloromethane–MeOH to give 5-(10,15,20-triphenylporphyrinatonickel(II))dimer (98 mg, 95%) as a purple solid; mp > 300 °C; R_f 0.6 (CH_2Cl_2–hexane, 1 : 2, v/v); δ_H(600 MHz, CD_2Cl_2) 7.73 (m, 19H), 8.11 (m, 15H), 8.60 (d, J 4.9 Hz, 4H), 8.86 (dd, J 4.9 Hz, 8H); δ_C(150.9 MHz, CD_2Cl_2) 115.6, 119.8, 119.9, 126.6, 126.7, 126.8, 127.6, 127.7, 131.8, 132.1 (m), 133.5, 133.6 (m), 140.6, 140.7, 142.4, 142.7, 143.2, 146.7; UV-vis (CH_2Cl_2) λ_{max} (lg ε) 413 (5.1), 443 (5.1), 535 (4.6) nm; HRMS ($C_{76}H_{46}N_8Ni_2$) calcd for [M^+] 1186.2567, found 1186.2552.

Results and discussion

Ni porphyrins represent a class of flexible molecules with a nearly square planar core conformation.[11] The molecular structure of the 5-(10,15,20-triphenylporphyrinatonickel(II))-dimer is shown in Fig. 1a. The molecule consists of two porphyrin macrocycles connected together through *meso*-positions by a single carbon-carbon bond.

At low surface coverage the NiTPP-dimer molecules form compact islands on the Ag(111) surface. Each island has an oblique close-packed structure and consists of NiTPP-dimer rows. Fig. 1b and c show typical unoccupied state STM images taken from approximately 0.5 monolayer (ML) of the NiTPP-dimer on the Ag(111) surface. The individual molecules appear as bright elongated protrusions (Fig. 1b) or two round shape protrusions (Fig. 1c) representing the individual porphyrin macrocycles within the dimer. The different contrast for the molecule in Fig. 1b and c can be attributed to the different tip to sample distance, which is smaller for the image in Fig. 1c, and different loop gain sensitivity (higher in the case of Fig. 1c). This leads to a more resolved image of the molecule showing two porphyrin macrocycles of the dimer separately (Fig. 1c). Each NiTPP-dimer molecule has a flat orientation on the surface with the macrocycle plane lying parallel to the substrate. The apparent size of an individual NiTPP-dimer molecule is approximately 2.7 nm long and 1.7 nm wide which is in good agreement with the expected size of the molecule.

The NiTPP-dimer molecules forming the border of the island appear to be less well resolved due to molecular movement (Fig. 1b). Individual molecules can be easily moved by the STM tip due to the relatively weak molecule-substrate interaction which is usual for low reactivity substrates such as Ag. Thus, NiTPP-dimer molecules are physisorbed on the Ag(111) surface and the molecule-substrate interaction occurs through the molecular π-electron system. The inter-molecular bonding appears to be stronger than the molecule-substrate

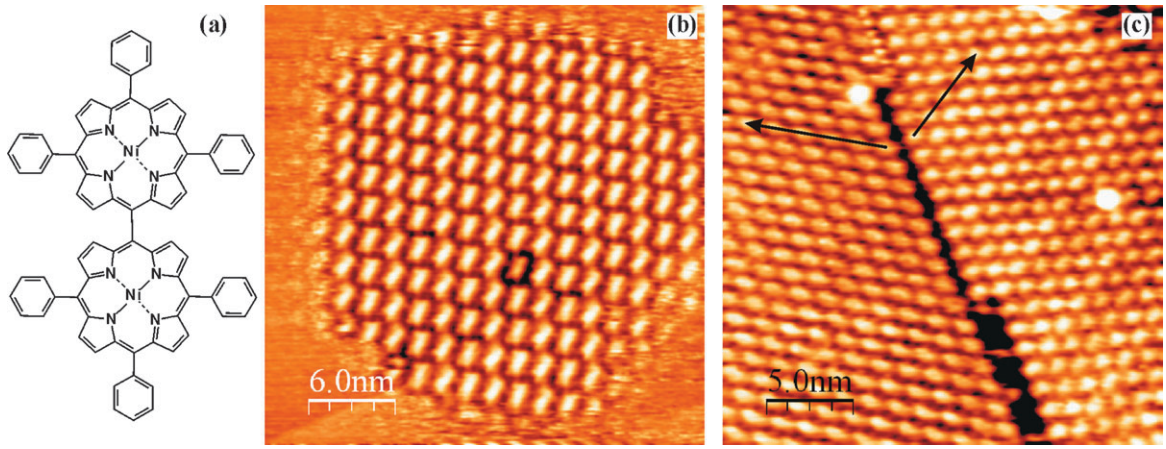

Fig. 1 Structural formula of the 5-(10,15,20-triphenylporphyrinatonickel(II))dimer (a). STM images obtained from approximately 0.5 ML of the NiTPPP-dimer on the Ag(111) surface: I_t = 0.10 nA, V_{sample} = −1.0 V, size 30 nm × 30 nm (b) and I_t = 0.18 nA, V_{sample} = −1.30 V, size 25 nm × 25 nm (c). Black arrows indicate close-packing directions of two molecular domains with an angle of 120° between them.

interaction. A competition between these interactions results in the formation of domains and domain boundaries (Fig. 1c). However, different domains (close-packing directions of these domains are indicated by arrows in Fig. 1c), observed at 0.5 ML coverage, follow the main crystallographic directions of the Ag(111) substrate. This indicates that the molecule-substrate interaction is strong enough to align the domains. It is further noted that the molecules desorb from the surface at a temperature of approximately 500 K which provides further evidence for a weakly bonded, physisorbed system.

All STM images of the NiTPP-dimer molecules on the Ag(111) surface show a close-packed structure of the self-assembled layer with a small separation between the molecules. This is a result of significant rotation of the phenyl rings attached to the porphyrin macrocycle. The plane of the phenyl rings is usually rotated by 50°–60° with respect to the macrocycle plane according to *ab initio* calculations, STM and X-ray absorption experiments.[22] Such rotation allows the NiTPP-dimer molecules to approach each other on the surface in a specific manner when intermolecular bonding occurs through π-electron system of the phenyl rings (π–π bonding).

At approximately 1 ML coverage the NiTPP-dimer molecules form large domains on the Ag(111) surface. At this preparation stage the surface was annealed at 325 K for 20 min after molecular deposition in order to assist molecular self-assembly. After annealing it is observed that each terrace is covered with a single molecular domain with terrace widths of up to 100 nm. Each domain has an oblique close-packed structure and consists of NiTPP-dimer rows. The unit cell parameters measured from STM images are a = 2.7 nm, b = 2.7 nm, γ = 70°. Fig. 2 shows typical STM images taken from approximately 1 ML of the NiTPP-dimer on the Ag(111) surface. From Fig. 2a it is clearly seen that single molecular domain occupies an entire substrate terrace. Furthermore, the angle between two molecular domains is equal to 120°. This indicates that the NiTPP-dimer domains grow along the main crystallographic directions of the Ag(111) substrate.

Fig. 2b shows a typical STM image obtained from 1 ML of the NiTPP-dimer on the A(111) surface. The rotated phenyl rings are seen as bright oval protrusions. Fig. 2c and d show

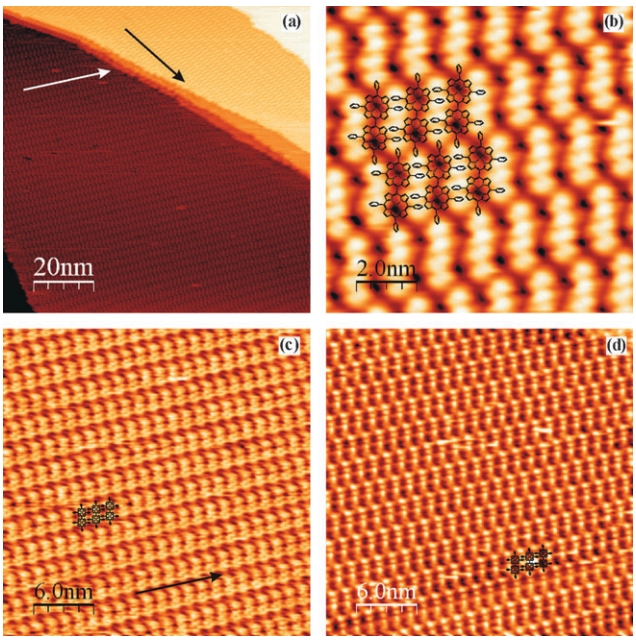

Fig. 2 STM images obtained from approximately 1 ML of the NiTPPP-dimer on the Ag(111) surface: I_t = 0.10 nA, V_{sample} = +0.73 V, size 100 nm × 100 nm (a), I_t = 0.1 nA, V_{sample} = −1.9 V, size 10 nm × 10 nm (b), I_t = 0.1 nA, V_{sample} = +0.65 V, size 30 nm × 30 nm (c) and I_t = 0.1 nA, V_{sample} = −0.65 V, size 30 nm × 30 nm (d). Arrows indicate close-packing directions of two molecular domains with an angle of 120° between them.

examples of images recorded simultaneously from the same area with a positive and negative sample bias, respectively. These STM images represent unoccupied (Fig. 2c) and occupied (Fig. 2d) electron states of the molecule. In Fig. 2c the NiTPP-dimers can be seen as a pairs of bright protrusions, representing the porphyrin macrocycles, with each protrusion showing a four-fold symmetry. In Fig. 2d the phenyl rings can be seen as bright dots, while the porphyrin macrocycle appears dark on the image preserving a four-fold symmetry. The different appearance of the molecules in Fig. 2c and d can be attributed to a difference in the electronic structure between the

porphyrin macrocycle and the phenyl substituents. According to the published electronic structure[23,24] of Ni porphyrin the first unoccupied molecular orbitals are localised in the macrocycle of the porphyrin and include unoccupied Ni 3d states. In this case electrons are tunnelling mainly into macrocycle states and not to the phenyl rings making the porphyrin core brighter than the substituents. When tunnelling occurs into a number of molecular orbitals localised both in the macrocycle and phenyl rings the latter appear to be brighter. This is due to rotated position of the phenyl rings which makes them higher than the porphyrin macrocycle. This simplified view does not take into account the interaction between the molecule and the substrate, however, it is assumed that this interaction is weak for the Ag(111) surface.

The LEED pattern obtained from 1 ML of the NiTPP-dimer on the Ag(111) surface shows three domains. The diffraction pattern for a single domain has an oblique unit cell (shown by rhombus in Fig. 3a) and confirms the structure observed in the STM images. The angle between each of the domains is equal to 120°. The upper insert in Fig. 3a is the LEED pattern obtained from the clean Ag(111) surface at a primary beam energy of 120eV. The reciprocal vectors a_1*, a_2* and a_3* drawn in Fig. 3a correspond to the [1$\bar{1}$0], [$\bar{1}$01] and [01$\bar{1}$] crystallographic directions of the Ag(111) substrate. The long diagonal of each rhombus lies parallel to one of these reciprocal vectors showing that the molecular domains align along the main crystallographic directions. Measurements of the lattice constants of the NiTPP-dimer overlayer, determined from a comparative analysis of LEED images from the overlayer and the substrate, are in agreement with the values obtained by STM. The clarity of the LEED pattern indicates the presence of a highly ordered NiTPP-dimer surface. A simulated LEED image created using the LEEDPat software[25] using a unit cell length of 2.7 nm with 70° between the lattice vectors (the bottom inset in Fig. 3a) is in excellent agreement with the experimental LEED image and provides further support for the unit cell dimensions obtained from both the STM and LEED data. The molecular layer is incommensurate with the substrate and may be represented by the following matrix:

$$\begin{pmatrix} 10.7 & 4.2 \\ 4.2 & 10.7 \end{pmatrix}$$

The registry of the molecular overlayer with respect to the underlying Ag(111) surface was determined using a combination of the LEED and STM results. The unit cell of the NiTPP-dimer overlayer (a = 2.7 nm) was found to be 4 per cent larger than nine times the unit cell length of the substrate (a_{sub} = 0.289 nm). This mismatch can be accommodated by displacing the position of the NiTPP-dimer molecule by three Ag(111) unit cell distance in the [1$\bar{1}$0] direction for every six unit cell displacements along the [10$\bar{1}$] direction, with corresponding displacements for the other two domains. In this case the long diagonals of the NiTPP-dimer unit cells for each of the three domains lie perfectly along the [1$\bar{1}$0], [01$\bar{1}$] and [$\bar{1}$01] directions of the Ag(111) surface in agreement with the LEED data. A corresponding model for the NiTPP-dimer overlayer is shown in Fig. 3b.

Fig. 4a shows a comparison between the normalized conductivity spectrum (dI/dV)/(I/V) and the z(V) spectrum recorded from the NiTPP-dimer overlayer on the Ag(111) surface. It is important to note that I(V) and z(V) spectroscopy are two different STM-based techniques providing similar information about the density of states of the material, which is probed as a function of voltage (sample bias) through changes in the tunnelling current (I(V)) or the tip height (z(V)).[7,26] The normalized conductivity spectrum was obtained by numerical differentiation of the I(V) spectrum and is proportional to the density of states. Each spectrum is the result of averaging over a few hundred spectra taken within an image using a grid of specified points. Spectra were recorded over the area of the image shown in Fig. 2b. These spectra provide averaged information about electronic structure of the

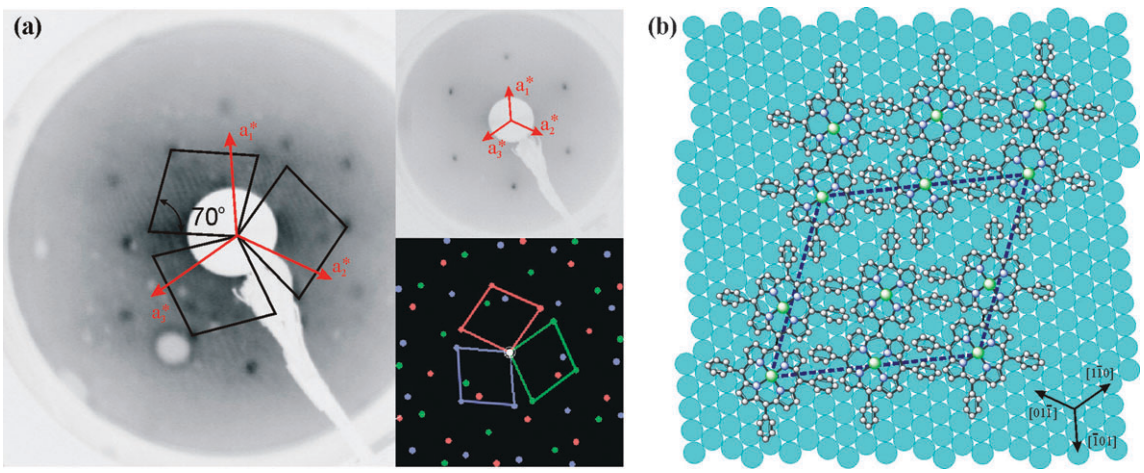

Fig. 3 LEED pattern from 1 ML of the NiTPP-dimer on the Ag(111) surface acquired at a primary beam energy of 13 eV (a). Three oblique diffraction patterns represent three NiTPP-dimer domains which grow along the [1$\bar{1}$0], [$\bar{1}$01] and [01$\bar{1}$] crystallographic directions of the substrate. Insets show LEED pattern from the clean Ag(111) surface acquired at a primary beam energy of 120 eV (top) and a simulated LEED image created using the LEEDPat software using a unit cell length of 2.7 nm with 70° between the lattice vectors (bottom). The main directions of the Ag(111) in reciprocal space are shown by the vectors a_1*, a_2* and a_3*. Schematic representation of the NiTPP-dimer overlayer on the Ag(111) surface (b).

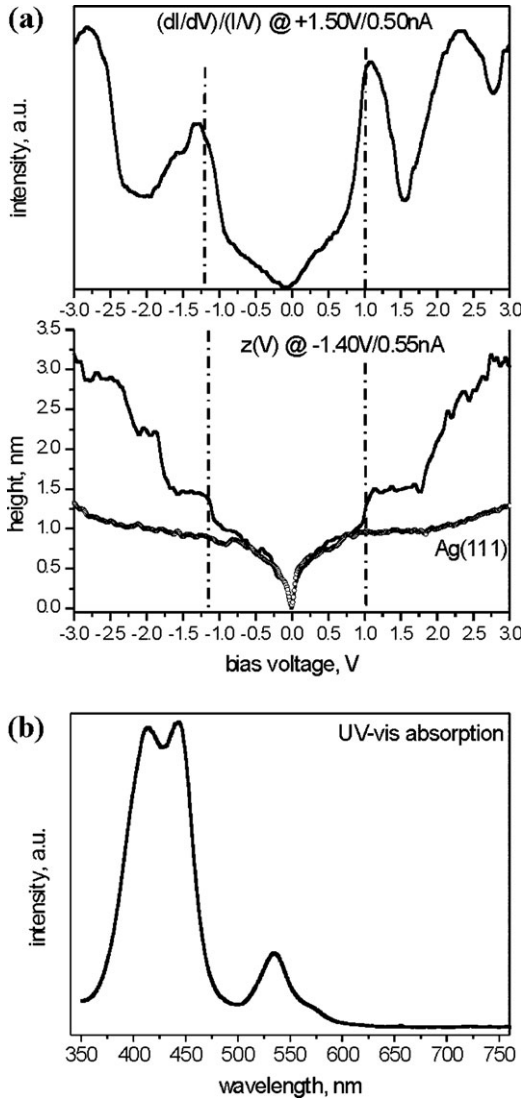

Fig. 4 Normalized conductivity $(dI/dV)/(I/V)$ spectrum (top) and $z(V)$ spectrum (bottom) recorded from 1 ML of the NiTPP-dimer on the Ag(111) surface (a). $z(V)$ spectrum of the clean Ag(111) surface is shown by open circles (a). A UV-vis absorption spectrum of the NiTPP-dimer (b).

dimer molecule. The normalized conductivity spectrum shows five prominent features: three peaks observed at −2.7 V, −1.5 V and −1.2 V and two peaks observed at 1.0 V and 2.3 V are related to occupied and unoccupied states, respectively. Furthermore, this spectrum shows good correlation with the features in the $z(V)$ spectrum in which characteristic steps are seen due to the increasing number of new channels (molecular orbitals) available for tunnelling as the bias voltage increases. These features are absent on the $z(V)$ curve obtained from the clean Ag(111) surface which proves that they are associated with the NiTPP-dimer.

The following peak assignment can be made by comparing these data with electronic structure calculations using density functional theory[23] and X-ray absorption spectroscopy results for Ni(II) porphyrins.[24] The peak observed at −1.2 eV is assigned to the highest occupied molecular orbital (HOMO) having a_{1g} symmetry. The unoccupied state situated at 1.0 eV is the lowest unoccupied molecular orbital (LUMO) having b_{1g} symmetry. The peak assignment was made keeping in mind that the Ni(II) porphyrin macrocycle has D_{4h} symmetry, which is preserved on the Ag(111) surface as shown in STM images, since molecule-substrate interaction is weak as discussed above. The chemical bonding of the nickel atom with four pyrrole rings in porphyrin macrocycle having D_{4h} symmetry results in the formation of four σ bonds due to in-plane mixing of ligand 2pσ states with Ni $3d_{z2}$ + 4s, $3d_{x2-y2}$ and $4p_{x,y}$ states, which are described by the a_{1g}, b_{1g} and e_u MOs respectively.[23,24] In this case the a_{1g} and b_{1g} MOs represent the HOMO and LUMO respectively. An additional π bonding of the metal atom with the ligands is fulfilled by a covalent interaction of the Ni $3d_{xz,yz}$ orbitals with the out-of-plane ligand 2p orbitals, which is accompanied by a charge transfer from the metal atom into the ligands (π-back donation).[24,27] This covalent bonding results in a π-MO of e_g symmetry. The HOMO–LUMO band gap of the NiTPP-dimer obtained from STS data is equal to 2.2 eV, which is in excellent agreement with theoretical calculations[23] and optical absorption spectroscopy results shown in Fig. 4b. The UV-vis absorption spectrum (Fig. 4b) shows a splitting of the Soret band which is characteristic of the dimeric porphyrin structure. The low-intensity shoulder in the Q-band at a wavelength of 585 nm represents the lowest energy transition between HOMO and LUMO. This value corresponds to an optical band gap of approximately 2.2 eV which is in excellent agreement with STS data.

Conclusions

In conclusion, the growth and ordering of the 5-(10,15,20-triphenylporphyrinatonickel(II))dimer on the Ag(111) surface have been investigated using STM, STS and LEED. A well-ordered molecular layer was obtained in which the NiTPP-dimer molecules have a flat orientation with the molecular planes lying parallel to the surface and form a close-packed structure with an oblique unit cell. STM and LEED data obtained from 1 ML of the NiTPP-dimer on the Ag(111) surface show the formation of three ordered domains which are aligned along the $[1\bar{1}0]$, $[\bar{1}01]$ and $[01\bar{1}]$ crystallographic directions of the substrate. STS data obtained from one monolayer of the NiTPP-dimer on the Ag(111) surface show good agreement with optical band gap measurements and density functional theory calculations.

Acknowledgements

This work was supported by the Irish Higher Education Authority PRTLI programme and by Science Foundation Ireland through the Research Frontiers Programme (grant number 06/RFP/PHY082 to A.A.C.) and a Science Foundation Ireland Research Professorship (grant number 04/RPI/B482 to M.O.S.). Y.N.S. gratefully acknowledges a Science Foundation Ireland UREKA 2007 award. STM topographic images were processed using WSxM software.[28]

Notes and references

1 A. Nitzan and M. A. Ratner, *Science*, 2003, **300**, 1384.
2 D. R. T. Zahn, G. N. Gavrila and G. Salvan, *Chem. Rev.*, 2007, **107**, 1161; M. O. Senge, M. Fazekas, E. G. A. Notaras, W. J. Blau, M. Zawadzka, O. B. Locos and E. M. N. Mhuircheartaigh, *Adv. Mater.*, 2007, **19**, 2737.
3 M. O. Senge, *Acc. Chem. Res.*, 2005, **38**, 733.
4 M. F. Craciun, S. Rogge and A. F. Morpurgo, *J. Am. Chem. Soc.*, 2005, **127**, 12210.
5 J. V. Barth, G. Costantini and K. Kern, *Nature*, 2005, **437**, 671; J. V. Barth, *Annu. Rev. Phys. Chem.*, 2007, **58**, 375; S. Stepanow, M. Lingenfelder, A. Dmitriev, H. Spillmann, E. Delvigne, N. Lin, X. Deng, C. Cai, J. V. Barth and K. Kern, *Nat. Mater.*, 2004, **3**, 229; J. A. Theobald, N. S. Oxtoby, M. A. Phillips, N. R. Champness and P. H. Beton, *Nature*, 2003, **424**, 1029; T. Yokoyama, S. Yokoyama, T. Kamikado, Y. Okuno and S. Mashiko, *Nature*, 2001, **413**, 619.
6 L. Grill, M. Dyer, L. Lafferentz, M. Persson, M. V. Peters and S. Hecht, *Nat. Nanotechnol.*, 2007, **2**, 687; F. Nishiyama, T. Yokoyama, T. Kamikado, S. Yokoyama, S. Mashiko, K. Sakaguchi and K. Kikuchi, *Adv. Mater.*, 2007, **19**, 117; H. Spillmann, A. Kiebele, M. Stöhr, T. A. Jung, D. Bonifazi, F. Cheng and F. Diederich, *Adv. Mater.*, 2006, **18**, 275.
7 S. A. Krasnikov, J. P. Beggan, N. N. Sergeeva, M. O. Senge and A. A. Cafolla, *Nanotechnology*, 2009, **20**, 135301; J. P. Beggan, S. A. Krasnikov, N. N. Sergeeva, M. O. Senge and A. A. Cafolla, *J. Phys.: Condens. Matter*, 2008, **20**, 015003; S. A. Krasnikov, C. J. Hanson, D. F. Brougham and A. A. Cafolla, *J. Phys.: Condens. Matter*, 2007, **19**, 446005.
8 X. Y. Zhu, *Surf. Sci. Rep.*, 2004, **56**, 1.
9 M. Eremtchenko, J. A. Schaefer and F. S. Tautz, *Nature*, 2003, **425**, 602.
10 P. Moriarty, *Rep. Prog. Phys.*, 2001, **64**, 297.
11 *The Porphyrin Handbook*, ed. K. M. Kadish, K. M. Smith and R. Guilard, Academic Press, San Diego, 2000, vol. 1–10; M. O. Senge and N. N. Sergeeva, *Angew. Chem., Int. Ed.*, 2006, **45**, 7492.
12 J. P. Collman and L. Fu, *Acc. Chem. Res.*, 1999, **32**, 455.
13 K. S. Suslick and S. van Deusen-Jeffries, in *Comprehensive Supramolecular Chemistry*, ed. K. S. Suslick, Elsevier, Oxford, 1996, vol. 5.
14 M. A. Schiavon, Y. Iamamoto, O. R. Nascimento and M. D. Assis, *J. Mol. Catal. A: Chem.*, 2001, **174**, 213.
15 H. L. Anderson, *Chem. Commun.*, 1999, 2323.
16 J. Chen, M. A. Reed, A. M. Rawlett and J. M. Tour, *Science*, 1999, **286**, 1550; A. Tsuda and A. Osuka, *Science*, 2001, **293**, 79.
17 J. A. W. Elemans, R. van Hameren, R. J. M. Nolte and A. E. Rowan, *Adv. Mater.*, 2006, **18**, 1251; R. van Hameren, P. Schon, A. M. van Buul, J. Hoogboom, S. V. Lazarenko, J. W. Gerritsen, H. Engelkamp, P. C. M. Christianen, H. A. Heus, J. C. Maan, T. Rasing, S. Speller, A. E. Rowan, J. A. W. Elemans and R. J. M. Nolte, *Science*, 2006, **314**, 1433; N. Katsonis, J. Vicario, T. Cudernac, J. Visser, M. M. Pollard and B. L. Feringa, *J. Am. Chem. Soc.*, 2006, **128**, 15537; W. Deng and K. W. Hipps, *J. Phys. Chem. B*, 2003, **107**, 10736.
18 M. Drobizhev, Y. Stepanenko, Y. Dzenis, A. Karotki, A. Rebane, P. N. Taylor and H. L. Anderson, *J. Am. Chem. Soc.*, 2004, **126**, 15352; M. Drobizhev, Y. Stepanenko, Y. Dzenis, A. Karotki, A. Rebane, P. N. Taylor and H. L. Anderson, *J. Phys. Chem. B*, 2005, **109**, 7223.
19 K. J. McEwan, P. A. Fleitz, J. E. Rogers, J. E. Slagle, D. G. McLean, H. Akdas, M. Katterle, I. M. Blake and H. L. Anderson, *Adv. Mater.*, 2004, **16**, 1933.
20 D. H. Yoon, S. B. Lee, K.-H. Yoo, J. Kim, J. K. Lim, N. Aratani, A. Tsuda, A. Osuka and D. Kim, *J. Am. Chem. Soc.*, 2003, **125**, 11062.
21 D. Bonifazi, A. Kiebele, M. Stöhr, F. Cheng, T. Jung, F. Diederich and H. Spillmann, *Adv. Funct. Mater.*, 2007, **17**, 1051; D. Bonifazi, H. Spillmann, A. Kiebele, M. de Wild, P. Seiler, F. Cheng, H.-J. Güntherodt, T. Jung and F. Diederich, *Angew. Chem., Int. Ed.*, 2004, **43**, 4759.
22 T. Yokoyama, S. Yokoyama, T. Kamikado and S. Mashiko, *J. Chem. Phys.*, 2001, **115**, 3814; M. P. de Jong, R. Friedlein, S. L. Sorensen, G. Öhrwall, W. Osikowicz, C. Tengsted, S. K. M. Jönsson, M. Fahlman and W. R. Salaneck, *Phys. Rev. B: Condens. Matter Mater. Phys.*, 2005, **72**, 035448; W. Auwärter, A. Weber-Bargioni, A. Riemann, A. Schiffrin, O. Gröning, R. Fasel and J. V. Barth, *J. Chem. Phys.*, 2006, **124**, 194708.
23 M.-S. Liao and S. Scheiner, *J. Chem. Phys.*, 2002, **117**, 205; A. Rosa, G. Ricciardi, E. J. Baerends and S. J. A. van Gisbergen, *J. Phys. Chem. A*, 2001, **105**, 3311.
24 S. A. Krasnikov, N. N. Sergeeva, M. M. Brzhezinskaya, A. B. Preobrajenski, Y. N. Sergeeva, N. A. Vinogradov, A. A. Cafolla, M. O. Senge and A. S. Vinogradov, *J. Phys.: Condens. Matter*, 2008, **20**, 235207; S. A. Krasnikov, A. B. Preobrajenski, N. N. Sergeeva, M. M. Brzhezinskaya, M. A. Nesterov, A. A. Cafolla, M. O. Senge and A. S. Vinogradov, *Chem. Phys.*, 2007, **332**, 318.
25 K. Hermann and M. A. van Hove, http://w3.rz-berlin.mpg.de/~hermann/LEEDpat/.
26 R. Feenstra, *Phys. Rev. B: Condens. Matter*, 1994, **50**, 4561; S. F. Alvarado, P. F. Seidler, D. G. Lidzey and D. D. C. Bradley, *Phys. Rev. Lett.*, 1998, **81**, 1082.
27 A. S. Vinogradov, A. B. Preobrajenski, A. Knop-Gericke, S. L. Molodtsov, S. A. Krasnikov, S. V. Nekipelov, R. Szargan, M. Hävecker and R. Schlögl, *J. Electron Spectrosc. Relat. Phenom.*, 2001, **114–116**, 813; A. S. Vinogradov, A. B. Preobrajenski, S. A. Krasnikov, T. Chassé, R. Szargan, A. Knop-Gericke, R. Schlögl and P. Bressler, *Surf. Rev. Lett.*, 2002, **9**, 359.
28 I. Horcas, R. Fernandez, J. M. Gomez-Rodriguez, J. Colchero, J. Gomez-Herrero and A. M. Baro, *Rev. Sci. Instrum.*, 2007, **78**, 013705.